Vacuum fluctuation effects on the ρ-meson mass and the one-ρ exchange potential at finite temperature and density

Yi-Jun Zhang,[1,2,*] Song Gao,[1,3,†] and Ru-Keng Su[4,1,‡]
[1]*Department of Physics, Fudan University, Shanghai 200433, China*
[2]*Department of Physics, University of Catania, 57 Corso Italia, I-95129 Catania, Italy*
[3]*Physics Department, McGill University, 3600 University Street, Montréal, QC, Canada H3A 2T8*
[4]*CCAST (World Laboratory), P.O. Box 8730, Beijing 100080, China*
(Received 24 February 1997)

Based on thermofield dynamics, the temperature- and density-dependent effective mass and screening mass of ρ meson have been calculated. The effects of vacuum fluctuation corrections through effective nucleon mass are examined. We have shown that vacuum fluctuations give an important correction to the self-energy of the ρ meson and lead to a reduction of the ρ-meson mass in hot and dense matter. The temperature and density dependence of one-ρ-meson exchange potential with vacuum fluctuation correction is also given. [S0556-2813(97)02612-5]

PACS number(s): 13.75.Cs, 12.40.Vv, 13.75.Lb, 14.40.Cs

I. INTRODUCTION

The study of the nuclear force plays an important role in understanding the physical properties of nuclear systems. When we extend our study to the high temperature and high density region, obviously, it is essential to determine the temperature and density dependence of nuclear force.

As is well known, the nuclear force can be understood on the basis of the exchange of various mesons. At large distances, the exchange of a pion gives the dominant contribution to the nuclear force. At intermediate distances, the dominant contribution arises from σ-meson or two-pion exchange, and at the short distances, it is generally believed that the dominant contribution of the nucleon-nucleon (NN) interaction comes from one-ρ-meson and one-ω-meson exchange. In our previous papers, by means of a finite temperature quantum field theory, after summing the temperature- and density-dependent vacuum polarization diagrams and the three-line vertex diagram which gives the correction of the coupling constant, we have extended the one-pion, one-σ-meson, and one-ω-meson exchange potential to finite temperature and density [1–4]. We have found that the attractive part of the NN interaction becomes weaker and the repulsive part becomes stronger when the temperature and/or density of the system increase. However, the study of the one-ρ-meson exchange potential (OREP) is still lacking. But the OREP in the NN interaction is very important because it has not only a vector coupling but also a tensor coupling, and, as was pointed out by Brown and Machleidt [5], unlike the ωNN interaction, the tensor coupling of the ρNN coupling is very strong. In our previous calculation [2], the tensor coupling of ωNN has been neglected. The first objective of this paper is to investigate the temperature and density dependence of the OREP; in particular, we will investigate the tensor coupling of ρNN in detail.

The second objective of this paper is to study the mass of the ρ meson in a hot and dense medium. There have been many papers published [7–13] which employ different models and different methods for studying the temperature and/or density effects of the ρ-meson mass, but unfortunately, the results are very different. Some of them, including that using an effective chiral Lagrangian [6], the vector dominance model [7], QCD sum rules and taking the mixing of vector and axial vector mesons into account [8], the π-π scattering amplitude [9], etc., have shown that the mass of the ρ meson increases with temperature. But the others [10–13] have shown the opposite results: The mass of the ρ meson decreases with temperature. The recent CERN experimental data on dileptons seem to support the reduction of the ρ-meson mass [14,15]. To clarify this puzzle, Shiomi and Hatsuda [16] and Song *et al.* [17] have shown that, for the ρNN vector and tensor coupling (VTC) model, even though the ρ-meson mass increases with temperature by summing the matter polarization diagrams, but if taking the vacuum fluctuation (VF) effect into account, i.e., changing the mass of the nucleon, m_N, in the Feynman propagator by its effective mass m_N^* in a medium and recalculate the vacuum polarization diagrams, one finds that the ρ-meson mass in a medium decreases with temperature or density. But in their calculations, the effective mass of the nucleon, m_N^*, is adopted from the mean field approximation results in the Walecka model (QHD-I) [18].

We hope to reexamine this problem by employing the Bonn potential (BP) model. This model has intermediate bosons π, σ, η, δ, ω, and ρ. In a previous paper [19], we extended the BP model to finite temperature and found the effective mass of the nucleon, m_N^*, reasonable. We will use this value to study the VF effects on the ρ-meson mass as well as the OREP. We will show that in this case the tensor potential of the OREP will change in a hot medium as in Ref. [20].

The organization of this paper is as follows. In Sec. II we will employ the VTC model to calculate the nucleon mass

*Electronic address: zhang@ct.infn.it (present)
†Electronic address: songgao@hep.physics.mcgill.ca
‡Electronic address: rksu@fudan.ac.cn

and the ρ-meson mass. We find that the effective mass of the nucleon almost decreases linearly with density at various fixed temperatures. The effective mass and the screening mass of the ρ meson all increase with temperature and density if the VF effect is neglected. But when one takes the VF effect into account the results are the opposite. In Sec. III, we will calculate the vertex correction of the ρNN coupling in a hot and dense medium. In Sec. IV, we will discuss the ρNN interaction at finite temperature and density and compare our result with that given by Brown and Rho.

II. ρ-MESON MASS IN A HOT AND DENSE MEDIUM

The interaction Lagrangian of the ρNN in a vector-tensor coupling model which plays an important role in the NN interaction is

$$\mathcal{L}_{\rho NN}=g_\rho\overline{\psi}\gamma_\mu\vec{\tau}\psi\cdot\vec{V}_\rho^\mu+\frac{f_\rho}{4m_N}\,\overline{\psi}\sigma_{\mu\nu}\vec{\tau}\cdot\psi(\partial^\mu\vec{V}_\rho^\nu-\partial^\nu\vec{V}_\rho^\mu), \tag{1}$$

where g_ρ and f_ρ are the vector and tensor coupling constants, m_N is the nucleon mass, ψ and $\vec{V}_\rho^\mu$ are, respectively, the nucleon field and ρ-meson field, $\sigma_{\mu\nu}=(i/2)[\gamma_\mu,\gamma_\nu]$, and $\vec{\tau}$ is the isospin operator. According to the arguments of Brown and Machleidt, the coupling constants are chosen as $f_\rho/g_\rho=6.1$ for a strong tensor coupling [5].

We use thermofield dynamics (TFD) [21] to discuss this problem. According to TFD, each field has double components and they lead to a 2×2 matrix propagator, but only the 1-1 component has a contribution to the self-energy. The 1-1 components of the nucleon and ρ meson are [2,3,21]

$$\Delta^{11}(k)=(\not{k}+m_N)\left\{\frac{1}{k^2-m_N^2+i\epsilon}+2\pi i N_F(k)\,\delta(k^2-m_N^2)\right\}, \tag{2}$$

$$D_\rho^{\mu\nu}(k)=\left(-g^{\mu\nu}+\frac{k^\mu k^\nu}{m_\rho^2}\right)\times\left[\frac{1}{k^2-m_\rho^2+i\epsilon}-2\pi i n_B(k)\,\delta(k^2-m_\rho^2)\right], \tag{3}$$

respectively, where $N_F(k)=[\theta(k_0)n_F(k)+\theta(-k_0)\overline{n_F}(k)]$, $\theta(k_0)$ is the step function, m_N, and m_ρ are the masses of nucleon and ρ meson in a vacuum, respectively, and

$$n_F(k)=\frac{1}{e^{\beta(|k_0|-\mu)}+1},\quad \overline{n_F}(k)=\frac{1}{e^{\beta(|k_0|+\mu)}+1}, \tag{4}$$

$$n_B(k)=\frac{1}{e^{\beta|k_0|}-1} \tag{5}$$

are the corresponding fermion, antifermion, and boson distribution functions. The self-energy of the ρ meson under a one-loop approximation reads [Fig. 1(a)]

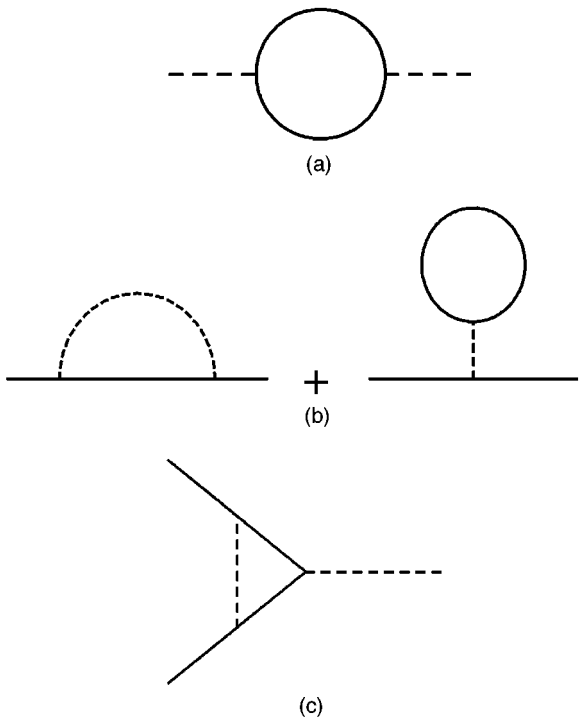

FIG. 1. Feynman diagrams: (a) The self-energy correction of the ρ meson; the solid line denotes the nucleon and the dashed lines the ρ meson. (b) Self-energy diagram correction of nucleon. (c) The three-line vertex correction.

$$\Pi_\rho^{\mu\nu}=-i\int\frac{d^4k}{(2\pi)^4}\,\mathrm{Tr}[\Gamma^\mu\Delta^{11}(k)\widetilde{\Gamma}^\nu\Delta^{11}(k+q)], \tag{6}$$

where

$$\Gamma^\mu=\left[g_\rho\gamma^\mu-\frac{f_\rho}{2m_N}i\sigma^{\mu\lambda}q_\lambda\right]\tau_i,$$

$$\widetilde{\Gamma}^\nu=\left[g_\rho\gamma^\nu+\frac{f_\rho}{2m_N}i\sigma^{\nu\lambda}q_\lambda\right]\tau_j. \tag{7}$$

It can easily be shown that when we substitute Eq. (2) into Eq. (6), $\Pi_\rho^{\mu\nu}$ can be separated into two parts; one refers to the naive zero temperature and density contribution, and the other depends on temperature and density, because the first term of the right-hand side of Eq. (2) is independent of temperature and density. The temperature and density part of $\Pi_\rho^{\mu\nu}$ is

$$\Pi_\rho^{\mu\nu}(q,T,\rho)=\int\frac{d^4k}{(2\pi)^3}T^{\mu\nu}\left\{\frac{\delta(k^2-m_N^2)}{(k+q)^2-m_N^2}N_F(k)+\frac{\delta[(k+q)^2-m_N^2]}{k^2-m_N^2}N_F(k+q)\right\}, \tag{8}$$

where

$$T^{\mu\nu}=\mathrm{Tr}\left\{\left[g_\rho\gamma^\mu+\frac{f_\rho}{2m_N}i\sigma^{\mu\lambda}q_\lambda\right](\not{k}+m_N)\left[g_\rho\gamma^\nu-\frac{f_\rho}{2m_N}i\sigma^{\nu\delta}q_\delta\right](\not{k}+\not{q}+m_N)\right\}$$
$$=4g_\rho^2\{k^\mu(k+q)^\nu+k^\nu(k+q)^\mu-g^{\mu\nu}[k\cdot(k+q)-m_N^2]\}-4g_\rho f_\rho(q^\mu q^\nu-q^2g^{\mu\nu})$$
$$-\frac{f_\rho^2}{m_N}\{q^\mu q^\nu(k^2-k\cdot q+m_N^2)-2k\cdot q(k^\mu q^\nu+q^\mu k^\nu)+2q^2k^\mu k^\nu+g^{\mu\nu}[2(k\cdot q)^2-q^2(k^2-k\cdot q-m_N^2)]\}. \quad (9)$$

Because of the self-energy correction, the propagator of the massive vector ρ meson in the hot and dense medium reads

$$D_\rho^{\mu\nu}(q)=-\frac{P_L^{\mu\nu}}{q^2-m_\rho^2-\Pi_L^\rho}-\frac{P_T^{\mu\nu}}{q^2-m_\rho^2-\Pi_T^\rho}, \quad (10)$$

where Π_L^ρ and Π_T^ρ are the longitudinal and the transverse components of the ρ-meson self-energy, respectively,

$$\Pi_L^\rho=-\frac{q^2}{\vec{q}^2}u_\mu u_\nu\Pi_\rho^{\mu\nu},\quad \Pi_T^\rho=\frac{1}{2}\left(\frac{q^2}{\vec{q}^2}u_\mu u_\nu-g_{\mu\nu}\right)\Pi_\rho^{\mu\nu}, \quad (11)$$

u_μ is the four-velocity of the medium, and in the medium rest frame $u_\mu=(1,\vec{0})$; $P_L^{\mu\nu}$ and $P_T^{\mu\nu}$ are projection tensors defined as

$$P_T^{00}=P_T^{0i}=P_T^{i0}=0,\quad P_T^{ij}=\delta^{ij}-q^iq^j/\vec{q}^2,$$
$$P_T^{\mu\nu}+P_L^{\mu\nu}=-g^{\mu\nu}+q^\mu q^\nu/q^2. \quad (12)$$

The effective mass of the ρ meson is defined as the pole of the propagator $D_\rho^{\mu\nu}$ in the limit $\vec{q}\to 0$ [4,6]. One can prove that, in the limit $\vec{q}\to 0$,

$$\Pi_L^\rho(q_0,\vec{q}\to 0)=\Pi_T^\rho(q_0,\vec{q}\to 0)=-\frac{1}{3}[\Pi^\rho]_\mu^\mu(q_0,\vec{q}\to 0). \quad (13)$$

Then the effective mass of the ρ meson is

$$m_\rho^{*2}=m_\rho^2+\Pi_L^\rho(q_0=m_\rho^*,\vec{q}\to 0). \quad (14)$$

From Eqs. (8), (11), and (13), we obtain

$$\Pi_L^\rho(q_0,\vec{q}\to 0,T,\rho)$$
$$=\frac{2g_\rho^2}{3\pi^2}(2I_2+m_N^2I_{3/2})$$
$$+\left(\frac{g_\rho^2}{3\pi^2}I_{3/2}+\frac{g_\rho f_\rho}{\pi^2}I_{3/2}-\frac{f_\rho^2}{3\pi^2}\frac{1}{m_N^2}I_4\right)q_0^2, \quad (15)$$

where

$$I_2=\int_0^\infty\frac{dx\,x^2}{\mathcal{E}_N(x)}[n_F(x)+\overline{n}_F(x)],$$
$$I_{3/2}=\int_0^\infty\frac{dx\,x^2}{\mathcal{E}_N^3(x)}[n_F(x)+\overline{n}_F(x)],$$
$$I_4=\int_0^\infty\frac{dx\,x^4}{\mathcal{E}_N^3(x)}[n_F(x)+\overline{n}_F(x)], \quad (16)$$

and $\mathcal{E}_N(x)=\sqrt{x^2+m_N^2}$. The effective mass m_ρ^* can be obtained from Eqs. (14)–(16) numerically.

However, there is another way to define the ρ-meson mass in a hot and dense medium. It is the so-called screening mass. The screening mass is defined as the inverse Debye screening length [3,4,6]. The equations for defining the longitudinal screening mass $m_{\rho L}^s$ and the transverse screening mass $m_{\rho T}^s$ of the ρ meson are

$$m_{\rho L}^s=[m_\rho^2+\Pi_L^\rho(0,\vec{q}\to 0)]^{1/2},$$
$$m_{\rho T}^s=[m_\rho^2+\Pi_T^\rho(0,\vec{q}\to 0)]^{1/2}. \quad (17)$$

We can prove

$$\Pi_L^\rho(0,\vec{q})=-\Pi_{00}^\rho(0,\vec{q}),$$
$$\Pi_T^\rho(0,\vec{q})=\frac{1}{2}\{\Pi_{00}^\rho(0,\vec{q})-[\Pi^\rho]_\mu^\mu(0,\vec{q})\} \quad (18)$$

and

$$m_{\rho L}^s=\left[H_L\left(m_\rho^2+\frac{4g_\rho^2}{\pi^2}I_2\right)\right]^{1/2},$$
$$m_{\rho T}^s=\left[H_T\left(m_\rho^2+\frac{g_\rho^2}{\pi^2}m_N^2I_{3/2}\right)\right]^{1/2}, \quad (19)$$

where

$$H_L=\left[1-\frac{g_\rho(g_\rho+2f_\rho)}{2\pi^2}I_{3/2}+\frac{f_\rho^2}{2\pi^2}\frac{I_4}{m_N^2}\right]^{-1},$$
$$H_T=\left[1-\frac{g_\rho(g_\rho+4f_\rho)}{4\pi^2}I_{3/2}-\frac{f_\rho^2}{4\pi^2}\left(2I_{3/2}+\frac{I_2+I_4}{m_N^2}\right)\right]^{-1}. \quad (20)$$

The numerical results of the effective mass m_ρ^* and screening masses $m_{\rho L}^s$, $m_{\rho T}^s$ vs T and ρ are shown in Figs. 2(a), 2(b) and Figs. 3(a), 3(b) by dashed lines, respectively, where

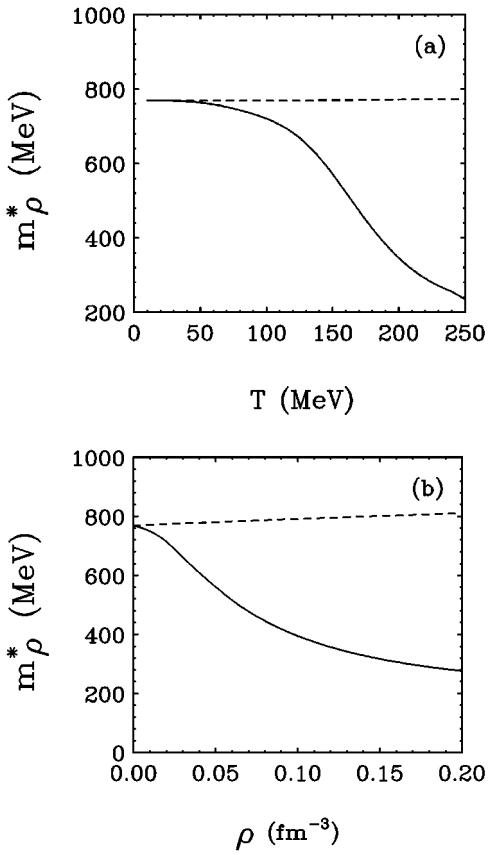

FIG. 2. (a) The temperature dependence of the effective mass of the ρ meson: the solid line with a vacuum fluctuation correction and the dashed line without. (b) Same as (a), but for density.

we choose the parameters as $m_N=939$ MeV, $m_\rho=769$ MeV, $g_\rho^2/4\pi=1.2$, and $f_\rho/g_\rho=6.1$. We see from Figs. 2(a), 2(b) and Figs. 3(a), 3(b) that m_ρ^*, $m_{\rho L}^s$, and $m_{\rho T}^s$ all increase with temperature and density, even though the increments for m_ρ^*, $m_{\rho L}^s$, and $m_{\rho T}^s$ are different.

Now let us examine the above calculations carefully. In the above calculations, we choose the mass of the nucleon, m_N, as its vacuum value, say, 939 MeV, and put it into $\Delta^{11}(k)$. It is only an approximation because in a hot and dense medium, the effective mass of the nucleon will shift from its vacuum value. A complete calculation must take the temperature and density dependence of the nucleon effective mass into account.

To consider the contribution of a hot and dense medium to the effective mass of the nucleon, we calculate the self-energy of the nucleon. The self-energy diagrams of the nucleon through ρ-meson exchange under a one-loop approximation are shown in Fig. 1(b). It can easily be seen that the contribution of tadpole diagrams from ρ-meson exchange to the nucleon self-energy is zero; then, according to the Feynman rules of TFD, the self-energy of the nucleon reads

$$\Sigma_N = i\int \frac{d^4k}{(2\pi)^4}\Gamma_\mu \Delta 11(k)\tilde{\Gamma}_\nu D_\rho^{\mu\nu}(k+p) = C-\gamma_0 p^0 A+\vec{\gamma}\cdot\vec{p}B. \tag{21}$$

Substituting Eqs. (2) and (3) into Eq. (21), after a straightforward calculation, we finally find

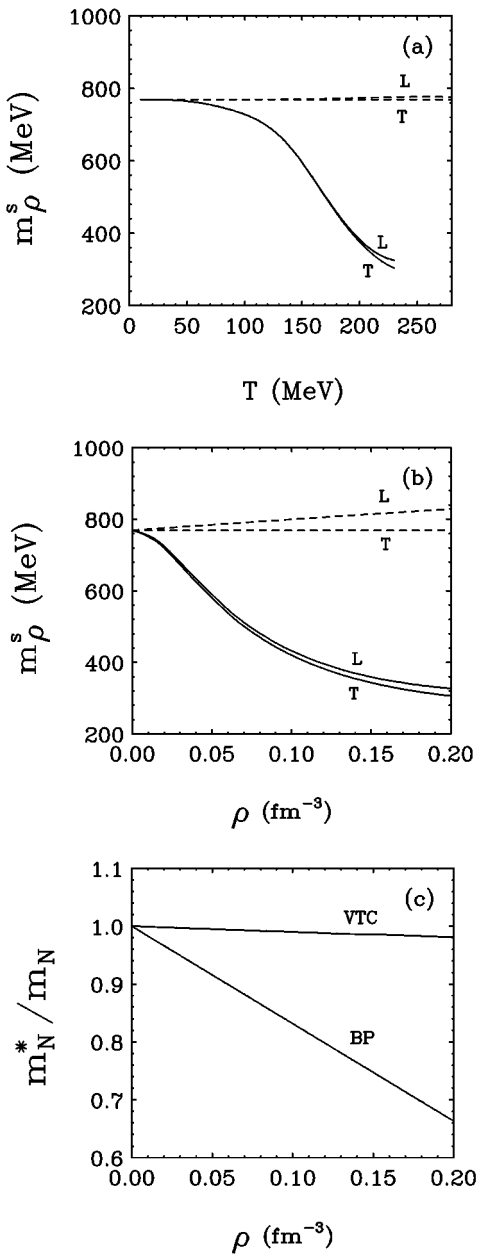

FIG. 3. (a) Same as Fig. 2(a), but for the screening mass of the ρ meson: L denotes the longitudinal part, and T denotes the transverse part. (b) Same as (a), but for density. (c) m_N^*/m_N vs density at $T=0$ for the VTC model and BP model.

$$m_N^* = m_N\left\{1+\frac{g_\rho^2}{4\pi^2}\left(3I(m_\rho)-\frac{I_2}{m_\rho}+\frac{6I_2^\rho}{4m_N^2-m_\rho}\right)+\frac{1}{4\pi}\frac{g_\rho f_\rho}{4m_N}\left(\frac{I_d}{m_\rho^2}+3I_E-\frac{6m_N}{4m_N^2-m_\rho^2}I_2^\rho\right)+\frac{1}{4\pi^2}\frac{f_\rho^2}{4m_N^2}\frac{1}{4m_\rho^2}\left[(2m_N^2-3m_\rho^2)I_2-2m_N I_d-3m_\rho^4 I(m_\rho)-\frac{2m_\rho^4}{4m_N^2-m_\rho^2}\right]\right\}, \tag{22}$$

where

$$I(m_\rho)=\int_0^\infty \frac{dx\,x^2}{\mathcal{E}_N(x)}\left[\frac{n_F(x)}{2m_N^2-m_\rho^2-2m_N\mathcal{E}_N(x)}+\frac{\overline{n_F}(x)}{2m_N^2-m_\rho^2+2m_N\mathcal{E}_N(x)}\right],$$

$$I_E=\int_0^\infty dx\,x^2\left[\frac{n_F(x)}{2m_N^2-m_\rho^2-2m_N\mathcal{E}_N(x)}-\frac{\overline{n_F}(x)}{2m_N^2-m_\rho^2+2m_N\mathcal{E}_N(x)}\right],$$

$$I_d=\int_0^\infty dx\;x^2[n_F(x)-\overline{n_F}(x)],\quad I_2^\rho=\int_0^\infty \frac{dx\,x^2}{\sqrt{x^2+m_\rho^2}}n_B(x). \tag{23}$$

The effective nucleon mass changes with densities for fixed temperatures ($T=0$ MeV) are shown in Fig. 3(c) by a solid line denoted by VTC. From Fig. 3(c), we find that the effective nucleon mass m_N^* decreases with density. The reductions of m_N^* are linear with density for fixed temperatures in low density regions.

Obviously, the reduction of m_N^* due to the exchange of a ρ meson in the VTC model is too small. The value of m_N^* at the saturation density is $m_N^*=0.98m_N$. In fact, the values of m_N^* depend on the model and the approximation considerably. We have shown that m_N^* reduces to $0.61m_N$ at the saturation density for the QHD-II model [4], $0.75m_N$ for a chiral σ-ω model [3], and $0.74m_N$ for the BP model [19]. The main contributions of the reduction of m_N^* come from the exchange of scalar mesons. The VTC model cannot lead to a reasonable reduction of m_N^*. To exhibit the effects of the reduction of m_N^* on the ρ-meson mass and OREP explicitly, hereafter we employ the BP model to study our problem. Since it is generally believed that the BP model can successfully describe the nuclear force, it includes not only ρ, ω, σ, π, η, and δ intermediate bosons, but also ρNN vector-tensor coupling, and adopting this model for further study would be suitable.

We study VF effects from the VTC model first. Substituting Eq. (22) into Eq. (2), we find the propagator of the nucleon as

$$\Delta^{11}(k)=(\gamma^\mu k_\mu^*+m_N^*)\left[\frac{1}{k^{*2}-m_N^{*2}+i\epsilon}+2\pi i N_F(k)\,\delta(k^{*2}-m_N^{*2})\right]. \tag{24}$$

Instead of m_N and the first term $(\not k+m_N)[1/(k^2-m_N^2+i\epsilon)]$ on the right-hand side of Eq. (2), we have m_N^* and $(\gamma^\mu k_\mu^*+m_N^*)[1/(k^{*2}-m_N^{*2}+i\epsilon)]$ in Eq. (24) where m_N^* depends on the temperature and density. Therefore, the zero temperature and density part of the self-energy of the ρ meson obtained from Eq. (6) becomes temperature and density dependent, which is

$$\Pi_{\rho v}^{\mu\nu}(q)=-i\int\frac{d^4k}{(2\pi)^4}\times\frac{\mathrm{Tr}\{\Gamma^\mu(\gamma^\mu k_\mu^*+m_N^*)\Gamma^\nu[\gamma^\mu(k_\mu^*+q_\mu^*)+m_N^*]\}}{(k^{*2}-m_N^{*2}+i\epsilon)[(k^*+q^*)^2-m_N^{*2}+i\epsilon]}. \tag{25}$$

$\Pi_{\rho v}^{\mu\nu}$ involves divergent integrals. These divergences may be rendered finite by the renormalization procedure, and these finite contributions are called VF corrections [16,17]. The effects of VF corrections can be calculated by the method of dimensional regularization, and using the subtraction procedure as in [16]. We obtain

$$\Pi_{\rho v}^{\mu\nu}(q)=(q^\mu q^\nu/q^2-g^{\mu\nu})\Pi_{\rho v}(q), \tag{26}$$

where

$$\Pi_{\rho v}(q)=\frac{g\rho^2}{\pi^2}q^2\int_0^1 dx\,x(1-x)\ln\frac{m_N^{*2}-q^2x(1-x)}{m_N^2-q^2x(1-x)}+\frac{g\rho f_\rho}{2\pi^2}\frac{m_N^*}{m_N}q^2\int_0^1 dx\;\ln\frac{m_N^{*2}-q^2x(1-x)}{m_N^2-q^2x(1-x)}+\frac{g\rho^2}{2\pi^2}\frac{1}{4m_N^2}q^2\int_0^1 dx[m_N^{*2}+q^2x(1-x)]\times\ln\frac{m_N^{*2}-q^2x(1-x)}{m_N^2-q^2x(1-x)}. \tag{27}$$

The total self-energy of the ρ meson reads

$$\Pi_\rho^{\mu\nu}(q)=\Pi_{\rho v}^{\mu\nu}(q)+\Pi_\rho^{\mu\nu}(q,T,\rho,m_N^*). \tag{28}$$

We use the above procedure to calculate the effective mass and the screening mass of the ρ meson by substituting m_N^* for m_N. The m_N^* is given by the BP model from our previous paper [19]. This m_N^* is more reasonable than that of the Walecka model because it considers more intermediate mesons, especially the ρ meson. Our results are shown in Figs. 2(a), 2(b), 3(a), 3(b), and 3(c) by the solid curves. We see from these figures that m_ρ^*, $m_{\rho L}^s$, and $m_{\rho T}^s$ decrease rapidly when employing the m_N^* of the BP model.

III. EFFECTIVE COUPLING OF ρNN

In a hot and dense medium, the coupling of the ρ meson to the nucleon will be modified by the temperature- and density-dependent vertex corrections. The Feynman diagram for the three-line vertex correction is shown in Fig. 1(c). According to the Feynman rules of TFD, the contribution of the three-line vertex correction is

$$\Lambda_\lambda=-i\int\frac{d^4k}{(2\pi)^4}\widetilde{\Gamma}_\mu\Delta^{11}(p'-k)\times\Gamma_\lambda\Delta^{11}(p-k)\Gamma_\nu g^{\mu\nu}D^{11}(k), \tag{29}$$

with $D^{11}(k)=1/(k^2-m_\rho^2+i\epsilon)-2\pi i n_B(k)\,\delta(k^2-m_\rho^2)$. Substituting the propagator of TFD into Eq. (29), using the same procedure as Refs. [1,3], we find that the temperature- and density-dependent part of Λ_λ is

$$\Lambda_\lambda(T,\rho) = -\int \frac{d^4k}{(2\pi)^3} \frac{T_\lambda}{[(p'-k)^2-m_N^2][(p-k)^2-m_N^2]} \delta(k^2-m_\rho^2) n_B(k) + \int \frac{d^4k}{(2\pi)^3} \frac{T_\lambda}{[(p-k)^2-m_N^2][k^2-m_\rho^2]} N_F(p'-k)\,\delta[(p'-k)^2-m_N^2)] + \int \frac{d^4k}{(2\pi)^3} \frac{T_\lambda}{[(p'-k)^2-m_N^2][k^2-m_\rho^2]} N_F(p-k)\,\delta[(p-k)^2-m_N^2)], \quad (30)$$

where

$$T_\lambda = \left[g_\rho \gamma_\mu + \frac{f_\rho}{2m_N} i\sigma_{\mu\alpha} k^\alpha \right] \tau_i (\not{p}' - \not{k} + m_N) \times \left[g_\rho \gamma_\lambda - \frac{f_\rho}{2m_N} i\sigma_{\lambda\delta} k^\delta \right] \tau_k (\not{p} - \not{k} + m_N) \times \left[g_\rho \gamma^\mu - \frac{f_\rho}{2m_N} i\sigma^{\mu\beta} k^\beta \right] \tau_j . \quad (31)$$

Substituting Eq. (31) into Eq. (30), after a straightforward calculation, we can rewrite Eq. (30) as

$$\Lambda_\lambda(T,\rho) = \left[g_\rho \gamma_\lambda \Lambda_g(T,\rho) - \frac{f_\rho}{2m_N} i\sigma_{\lambda\delta} q^\delta \Lambda_f(T,\rho) \right] \tau_k , \quad (32)$$

and the full vertex can be written as

$$\Gamma_\lambda(T,\rho) = \Gamma_\lambda + \Lambda_\lambda(T,\rho) = g_\rho(T,\rho)\,\gamma_\lambda - \frac{1}{2m_N} f_\rho(T,\rho)(i\sigma_{\lambda\delta} q^\delta). \quad (33)$$

From Eqs. (7), (32), and (33), we can define the effective coupling constant of ρNN vector and tensor couplings due to the finite-temperature and -density vertex correction as

$$g_\rho^* \equiv g_\rho(T,\rho) = g_\rho[1+\Lambda_g(T,\rho)],$$

$$f_\rho^* \equiv f_\rho(T,\rho) = f_\rho[1+\Lambda_f(T,\rho)], \quad (34)$$

where

$$\Lambda_g(T,\rho) = \frac{g_\rho^2}{2\pi^2} \int d|\vec{k}| [f_1(\mathcal{E}_\rho) + \tfrac{1}{2} f_2(\mathcal{E}_k)] - \frac{g_\rho f_\rho}{2\pi^2} \int d|\vec{k}| [f_3(\mathcal{E}_\rho) + \tfrac{1}{2} f_4(\mathcal{E}_k)] - \frac{f_\rho^2}{2\pi^2} \int d|\vec{k}| [f_3(\mathcal{E}_\rho) + \tfrac{1}{2} f_4(\mathcal{E}_k)], \quad (35a)$$

$$\Lambda_f(T,\rho) = \frac{g_\rho^2}{\pi^2} \int d|\vec{k}| [f_5(\mathcal{E}_\rho) - \tfrac{1}{4} f_6(\mathcal{E}_k)] - \frac{g_\rho f_\rho}{2\pi^2} \int d|\vec{k}| [f_7(\mathcal{E}_\rho) + \tfrac{1}{2} f_8(\mathcal{E}_k)] - \frac{f_\rho^2}{2\pi^2} \int d|\vec{k}| [f_3(\mathcal{E}_\rho) + \tfrac{1}{2} f_4(\mathcal{E}_k)], \quad (35b)$$

and $\mathcal{E}_k = \sqrt{|\vec{k}|^2 + m_N^2}$, $\mathcal{E}_\rho = \sqrt{|\vec{k}|^2 + m_\rho^2}$, and the functions $f_1 - f_8$ are given in the Appendix. The numerical results of the coupling constants vs temperature or density for a fixed density $\rho = 0$ or for a fixed temperature $T = 0$ are shown in Fig. 4(a) and Fig. 4(b) where the solid lines refer to g_ρ^*/g_ρ and the dashed lines to f_ρ^*/f_ρ, respectively. From Fig. 4(a) and Fig. 4(b), we find that the coupling constants decrease as T or ρ increases.

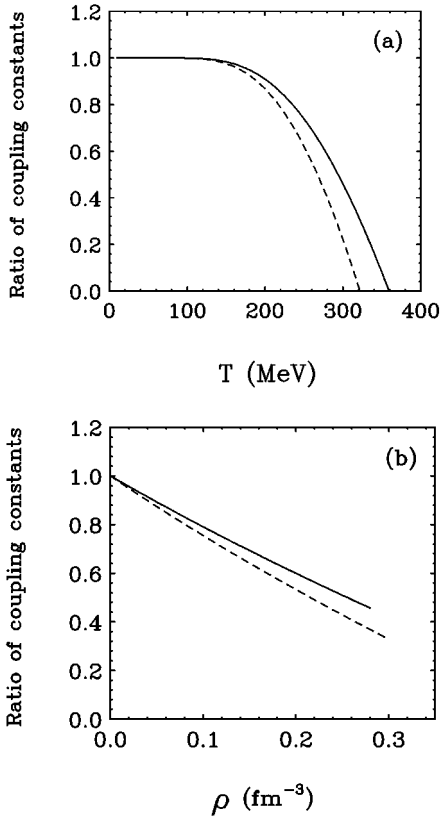

FIG. 4. (a) The ratio of coupling constants vs temperature (fixed $\rho = 0$); the solid line refers to g_ρ^*/g_ρ and the dashed line to f_ρ^*/f_ρ. (b) Same as (a), but vs density (fixed $T = 0$).

TABLE I. Symmetry energy (in MeV unit) for the Walecka model and the Walecka model with a free and effective ρ-meson vector-tensor coupling at different temperatures.

Models	$T=0$ MeV	$T=10$ MeV	$T=20$ MeV
Walecka model (WM)	43.51	45.39	46.64
WM with effective ρNN VTC	57.23	59.54	61.73
WM with free ρNN VTC	79.90	84.05	89.15

Of course, instead of m_N, we can use its value in a hot medium, m_N^*, in the above calculation to discuss VF effects on the effective coupling. But it can be shown that compared to the vacuum polarization diagrams, the VF effects on the three-line vertex and then to the effective coupling are small, and can be neglected.

To see the importance of the temperature and density dependences of the VTC effective coupling, we hereafter calculate the changes of symmetry energy (SE) brought by the VTC effective coupling in the mean field approximation. For simplicity, we first employ the Walecka model [18] to calculate the SE and then repeat the calculation by adding ρ-meson VTC. The results are listed in Table I. We can see from Table I that when the ρ-meson VTC is added to the Walecka model, the SE's change considerably. Though the SE's obtained here are somewhat larger than those given in Ref. [22], they are still near to the empirical values given by other papers [18,23]. However, if the free VTC is used instead of an effective one, the changes of SE's are too large. This is because medium effects suppress the effective couplings.

IV. ρNN INTERACTION POTENTIAL

We now discuss the NN interaction through one-ρ-meson exchange in a hot and dense medium by taking into account the self-energy and vertex corrections. The OREP becomes temperature and density dependent because of the dependence of the screening mass and the effective coupling constants of the ρ meson on temperature and density, which are given in Secs. II and III. Following treatments similar to our previous works [1–4], the OREP at finite temperature and density under the nonrelativistic approximation can be found as

$$V_\rho(r)=V_\rho\vec{\tau}_1\cdot\vec{\tau}_2, \tag{36}$$

with

$$\begin{aligned}V_\rho=&\frac{H_L}{4\pi}m_{\rho L}^s\left\{g_\rho^{*2}\left[\left(1+\frac{m_{\rho L}^{s2}}{4m_N^2}\right)Y(x_L)-\frac{1}{2}Z_1(x_L)\vec{L}\cdot\vec{S}\right]+\frac{1}{2}g_\rho^*f_\rho^*\left[\left(\frac{m_{\rho L}^s}{m_N}\right)^2Y(x_L)-2Z_1(x_L)\vec{L}\cdot\vec{S}\right]\right.\\&+\frac{H_T}{4\pi}m_{\rho T}^s\left\{g_\rho^{*2}\left[\frac{m_{\rho T}^{s2}}{4m_N^2}\left(1-\frac{m_{\rho T}^{s2}}{16m_N^2}\right)Y(x_T)-\left(1-\frac{m_{\rho T}^{s2}}{16m_N^2}\right)Z_1(x_T)\vec{L}\cdot\vec{S}+\frac{1}{6}\left(\frac{m_{\rho T}^s}{m_N}\right)^2Y(x_T)(\vec{\sigma}_1\cdot\vec{\sigma}_2)-\frac{1}{12}Z(x_T)S_{12}\right]\right.\\&\left.\left.+g_\rho^*f_\rho^*\left[\frac{1}{3}\left(\frac{m_{\rho T}^s}{m_N}\right)^2Y(x_T)(\vec{\sigma}_1\cdot\vec{\sigma}_2)-Z_1(x_T)\vec{L}\cdot\vec{S}-\frac{1}{6}Z(x_T)S_{12}\right]+\frac{f_\rho^{*2}}{6}\left[\left(\frac{m_{\rho T}^s}{m_N}\right)^2Y(x_T)(\vec{\sigma}_1\cdot\vec{\sigma}_2)-\frac{1}{2}Z(x_T)S_{12}\right]\right\},\end{aligned} \tag{37}$$

where, $x_L=m_{\rho L}^s r$, $x_T=m_{\rho T}^s r$, and

$$Y(x_i)=e^{-x_i}/x_i,\quad Z_1(x_i)=\left(\frac{m_{\rho i}^s}{m_N}\right)^2\left(\frac{1}{x_i}+\frac{1}{x_i^2}\right)Y(x_i),$$

$$Z(x_i)=\left(\frac{m_{\rho i}^s}{m_N}\right)^2\left(1+\frac{3}{x_i}+\frac{3}{x_i^2}\right)Y(x_i),$$

$$S_{12}=\frac{3(\vec{\sigma}_1\cdot\vec{r})(\vec{\sigma}_2\cdot\vec{r})}{r^2}-\vec{\sigma}_1\cdot\vec{\sigma}_2, \tag{38}$$

with $i=L,T$. In the meson-nucleon interaction theory, it is necessary to apply a form factor

$$\left[\frac{\Lambda_\alpha^2-m_\alpha^2}{\Lambda_\alpha^2-(\vec{p}'-\vec{p})^2}\right]^{n_\alpha}$$

to the meson-nucleon vertex because of the (quark) substructure of the nucleon and mesons [18,24]. Considering the effect of the form factor of the ρ-meson-nucleon vertex and taking $n_\rho=1$ [18,24], we obtain the OREP as

$$\begin{aligned}V_\rho(r)=&V_\rho(m_{\rho i}^*,r)-\frac{\Lambda_2^2-m_{\rho i}^{*2}}{\Lambda_2^2-\Lambda_1^2}V_\rho(\Lambda_1,r)\\&-\frac{\Lambda_2^1-m_{\rho i}^{*2}}{\Lambda_2^2-\Lambda_1^2}V_\rho(\Lambda_2,r)\quad(i=L,T),\end{aligned} \tag{39}$$

where $\Lambda_1=\Lambda_\rho+\epsilon$ and $\Lambda_2=\Lambda_\rho-\epsilon$ with $\epsilon/\Lambda_\rho\ll1$, Λ_ρ the cutoff mass of the ρNN vertex. As in Ref. [24], we choose $\Lambda=1.2$ GeV and $\epsilon=10$ MeV.

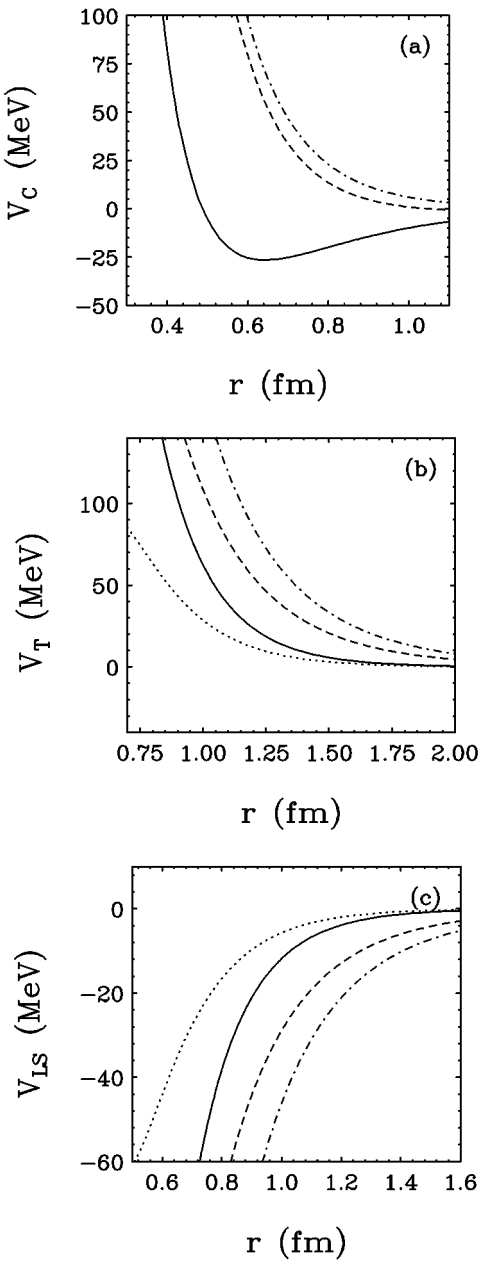

FIG. 5. (a) The central part of one-ρ-meson exchange potential for the $I=1$, $S=0$ state, where the solid line refers to $T=0$, $\rho=0$, the dot-dashed line to $T=200$ MeV, $\rho=0$, and the dashed line to $T=0$, $\rho=0.1$ fm^{-3}. (b) Same as (a), but for the tensor part ($I=0$, $S=1$). The dotted line corresponds to $T=0$, $\rho=0.1$ fm^{-3} without a VF correction. (c) Same as (b), but for the spin-orbit part.

The OREP expressed by Eqs. (36)–(39) can be separated into different components:

$$V_\rho(r)=V_C(r)+V_T(r)S_{12}+V_{LS}(r)\vec{L}\cdot\vec{S}, \qquad (40)$$

where $V_C(r)$, $V_T(r)$, and $V_{LS}(r)$ are, respectively, the central, tensor, and spin-orbit nuclear potential through one-ρ-meson exchange. The results for the central part $V_C(r)$ (isospin $I=1$, spin $S=0$ state) at different temperatures and densities are shown in Fig. 5(a), where the solid line refers to $T=0$, $\rho=0$ and the dot-dashed line to $T=200$ MeV, $\rho=0$ as well as the dashed line to $T=0$, $\rho=0.1$ fm^{-3}. We find that the temperature and density play the same role which makes the repulsive force of the OREP become stronger.

The results for the tensor part $V_T(r)$ ($I=0$, $S=1$) at different temperatures and densities are shown in Fig. 5(b), where the solid line refers to $T=0$, $\rho=0$, the dot-dashed line to $T=200$ MeV, $\rho=0$, and the dashed line to $T=0$, $\rho=0.1$ fm^{-3}. For both dot-dashed and dashed curves, we have taken the VF into account. It is of interest to compare our results with those obtained earlier by Brown and Rho [20]. Based on a scaling conjecture of the effective masses of the nucleon and ρ meson in a medium [25] and the correction of the form factor of the OREP, they found an enhancement of the tensor potential of the OREP in a medium. We restudy this problem by a detailed calculation of vacuum polarization diagrams and vertex correction diagrams of ρ mesons and nucleons under a one-loop approximation, and obtain the density and the temperature dependences of the tensor potential of the OREP. We see from Fig. 5(b) that our results are in qualitative agreement with that of Brown and Rho. An enhancement of $V_T(r)$ due to density and/or temperature is found. In order to explain our results clearly, we show a $V_T(r)$ vs r curve for $T=0$, $\rho=0.1$ fm^{-3} but without a VF correction by a dotted line in Fig. 5(b) simultaneously. We see that the dotted curve of $V_T(r)$ becomes lower than the solid line, i.e., the vacuum tensor potential. Instead of enhancement, a declination has been found. The reason for the declination of the dotted line comes from the increment of the ρ-meson mass. As shown in Figs. 2(a) and 2(b), when we neglect the VF, the ρ-meson mass will increase with temperature and density, and it makes $V_T(r)$ decrease. But if we consider the VF, an opposite result for the ρ-meson mass and then $V_T(r)$ will happen.

Finally, we show the temperature and density dependence of the spin-orbit nuclear potential through one-ρ-meson exchange ($I=1$, $S=0$) in Fig. 5(c) where the solid line refers to $T=0$, $\rho=0$, the dot-dashed line to $T=200$ MeV, $\rho=0$, and the dashed line to $T=0$, $\rho=0.1$ fm^{-3}. For comparison, we show the $V_{LS}(r)$ curve without a VF correction for $T=0$, $\rho=0$ fm^{-3} by dotted line in Fig. 5(c) simultaneously. Because of same reason, we find the same behavior as that of Fig. 5(b).

In summary, employing the vector-tensor ρNN coupling model, Bonn potential model and thermofield dynamics, we have calculated the effective mass and the screening mass of the ρ meson as well as the effective mass of the nucleon under a one-loop approximation, and studied VF effects. Of course the vacuum fluctuation effect can also come from other baryon-antibaryon vacuum polarization. But since we focus our attention only on the nuclei, in particular, the nuclear force and, usually, its dominant contribution comes from the exchange of mesons between nucleons; here we consider the nucleon-antinucleon vacuum polarization only. The baryon-antibaryon VF may be important in the baryon interaction. We have shown that the contributions of the VF to the mass of the ρ meson and to the OREP are very impor-

tant. Any calculations without a VF correction for the meson mass in a hot medium are incomplete.

Finally, we hope to point out that we can use our temperature- and density-dependent potential, for example, the extended Bonn potential, to discuss the thermodynamical properties of symmetric or asymmetric nuclear matter, for example, its phase transition, Coulomb instability, equation of state, and the critical point, as was previously done in Ref. [26]. Work on this topic is in progress.

ACKNOWLEDGMENTS

One of the authors (Y.J.Z.) would like to thank Dr. W. Zuo for helpful discussion. This work was supported in part by NNSF of China.

APPENDIX

The functions used in the integrals for the vertices corrections are as follows:

$$f_1(\mathcal{E}_\rho)=\frac{|\vec{k}|^2}{\mathcal{E}_\rho}\left[\frac{2m_N^2-4m_N\mathcal{E}_\rho+m_\rho^2}{(m_\rho^2-2m_N\mathcal{E}_\rho)^2}+\frac{2m_N^2+4m_N\mathcal{E}_\rho+m_\rho^2}{(m_\rho^2+2m_N\mathcal{E}_\rho)^2}\right]n_B, \tag{A1}$$

$$f_2(\mathcal{E}_k)=\frac{2(m_N^2-m_\rho^2)\mathcal{E}_N^2+8m_N\mathcal{E}_N^3-m_N(6m_N^2-m_\rho^2)\mathcal{E}_N+m_N^2m_\rho^2-4m_N^4}{\mathcal{E}_N(2m_N^2-m_\rho^2-2m_N\mathcal{E}_N)^2}n_F$$
$$+\frac{2(m_N^2-m_\rho^2)\mathcal{E}_N^2-8m_N\mathcal{E}_N^3+m_N(6m_N^2-m_\rho^2)\mathcal{E}_N+m_N^2m_\rho^2-4m_N^4}{\mathcal{E}_N(2m_N^2-m_\rho^2+2m_N\mathcal{E}_N)^2}\overline{n}_F, \tag{A2}$$

$$f_3(\mathcal{E}_\rho)=\frac{|\vec{k}|^2}{\mathcal{E}_\rho}\left[\frac{m_\rho^2}{(m_\rho^2-2m_N\mathcal{E}_\rho)^2}+\frac{m_\rho^2}{(m_\rho^2+2m_N\mathcal{E}_\rho)^2}\right]n_B, \tag{A3}$$

$$f_4(\mathcal{E}_k)=\frac{2(m_N^2+m_\rho^2)\mathcal{E}_N^2-m_N(4m_N^2-m_\rho^2)\mathcal{E}_N+2m_N^4-3m_N^2m_\rho^2}{\mathcal{E}_N(2m_N^2-m_\rho^2-2m_N\mathcal{E}_N)^2}n_F+\frac{2(m_N^2+m_\rho^2)\mathcal{E}_N^2+m_N(4m_N^2-m_\rho^2)\mathcal{E}_N+2m_N^4-3m_N^2m_\rho^2}{\mathcal{E}_N(2m_N^2-m_\rho^2+2m_N\mathcal{E}_N)^2}\overline{n}_F, \tag{A4}$$

$$f_5(\mathcal{E}_\rho)=\frac{|\vec{k}|^2}{\mathcal{E}_\rho}\left[\frac{m_N^2-2m_N\mathcal{E}_\rho}{(m_\rho^2-2m_N\mathcal{E}_\rho)^2}+\frac{m_N^2+2m_N\mathcal{E}_\rho}{(m_\rho^2+2m_N\mathcal{E}_\rho)^2}\right]n_B, \tag{A5}$$

$$f_6(\mathcal{E}_k)=\frac{8m_N^2\mathcal{E}_N^2-8m_N\mathcal{E}_N^3+2m_N(m_N^2+m_\rho^2)\mathcal{E}_N-2m_N^4-2m_N^2m_\rho^2}{\mathcal{E}_N(2m_N^2-m_\rho^2-2m_N\mathcal{E}_N)^2}n_F$$
$$+\frac{8m_N^2\mathcal{E}_N^2+8m_N\mathcal{E}_N^3-2m_N(m_N^2+m_\rho^2)\mathcal{E}_N-2m_N^4-2m_N^2m_\rho^2}{\mathcal{E}_N(2m_N^2-m_\rho^2+2m_N\mathcal{E}_N)^2}\overline{n}_F, \tag{A6}$$

$$f_7(\mathcal{E}_\rho)=\frac{|\vec{k}|^2}{\mathcal{E}_\rho}\left[\frac{m_\rho^2+4m_N\mathcal{E}_\rho}{(m_\rho^2-2m_N\mathcal{E}_\rho)^2}+\frac{m_\rho^2-4m_N\mathcal{E}_\rho}{(m_\rho^2+2m_N\mathcal{E}_\rho)^2}\right]n_B, \tag{A7}$$

$$f_8(\mathcal{E}_k)=\frac{2(7m_N^2+m_\rho^2)\mathcal{E}_N^2-8m_N\mathcal{E}_N^3-m_N(4m_N^2-3m_\rho^2)\mathcal{E}_N-2m_N^4-5m_N^2m_\rho^2}{\mathcal{E}_N(2m_N^2-m_\rho^2-2m_N\mathcal{E}_N)^2}n_F$$
$$+\frac{2(7m_N^2+m_\rho^2)\mathcal{E}_N^2+8m_N\mathcal{E}_N^3+m_N(4m_N^2-3m_\rho^2)\mathcal{E}_N-2m_N^4-5m_N^2m_\rho^2}{\mathcal{E}_N(2m_N^2-m_\rho^2+2m_N\mathcal{E}_N)^2}\overline{n}_F. \tag{A8}$$

[1] R. K. Su and G. T. Zheng, J. Phys. G **16**, 203 (1990); R. K. Su, G. T. Zheng, and G. G. Siu, *ibid.* **19**, 79 (1993); Z. X. Qian, C. G. Su, and R. K. Su, Phys. Rev. C **47**, 877 (1993); R. K. Su, Z. X. Qian, and G. T. Zheng, J. Phys. G **17**, 1785 (1991).

[2] S. Gao, R. K. Su, and P. K. N. Yu, Phys. Rev. C **49**, 40 (1994).

[3] R. K. Su, S. J. Yang, S. Gao, and P. K. N. Yu, J. Phys. G **20**, 1757 (1994); S. Gao, Y. J. Zhang, and R. K. Su, Nucl. Phys. **A593**, 362 (1995).

[4] S. Gao, Y. J. Zhang, and R. K. Su, Chin. Phys. Lett. **13**, 89 (1996); S. Gao, Y. J. Zhang, and R. K. Su, Phys. Rev. C **52**, 381 (1995).
[5] G. E. Brown and R. Machleidt, Phys. Rev. C **50**, 1731 (1994).
[6] C. Song, Phys. Rev. D **48**, 1375 (1993); **49**, 1556 (1994).
[7] C. Gale and J. I. Kapusta, Nucl. Phys. **B357**, 65 (1991); S. Gao, Y. J. Zhang, and R. K. Su, J. Phys. G **21**, 1665 (1995).
[8] M. Dey, V. L. Eletsky, and B. L. Ioffe, Phys. Lett. B **252**, 620 (1990).
[9] C. A. Dominguez, Z. Phys. C **59**, 63 (1993).
[10] T. Hatsuda and S. H. Lee, Phys. Rev. C **46**, R34 (1992).
[11] T. Hatsuda, Y. Koike, and S. H. Lee, Phys. Rev. D **47**, 1225 (1993); Nucl. Phys. **B394**, 221 (1993).
[12] C. Adami and G. E. Brown, Phys. Rev. D **46**, 478 (1992).
[13] G. E. Brown, Nucl. Phys. **A522**, 397c (1991); **A488**, 695c (1988); Z. Phys. C **38**, 291 (1988).
[14] G. Agakichiev *et al.*, Phys. Rev. Lett. **75**, 1272 (1995).
[15] G. Q. Li, C. M. Ko, and G. E. Brown, Phys. Rev. Lett. **75**, 4007 (1995).
[16] H. Shiomi and T. Hatsuda, Phys. Lett. B **334**, 281 (1994).
[17] C. Song, P. W. Xia, and C. M. Ko, Phys. Rev. C **52**, 408 (1995).
[18] B. D. Serot and J. D. Walecka, Adv. Nucl. Phys. **16**, 1 (1986).
[19] S. Gao, Y. J. Zhang, and R. K. Su, Phys. Rev. C **53**, 1098 (1996).
[20] G. E. Brown and M. Rho, Phys. Lett. B **237**, 3 (1990).
[21] H. Umezawa, H. Matsumoto, and M. Tachiki, *Thermo Field Dynamics and Condensed States* (North-Holland, Amsterdam, 1982).
[22] Y. Sugahara and H. Toki, Nucl. Phys. **A579**, 557 (1994), and references therein.
[23] A. Bohr and B. R. Mottelson, *Nuclear Structure* (Benjamin, New York, 1969).
[24] R. Machleidt, K. Holinde, and Ch. Elster, Phys. Rep. **149**, 1 (1987); R. Machleidt, Adv. Nucl. Phys. **19**, 189 (1989).
[25] G. E. Brown and M. Rho, Phys. Rev. Lett. **66**, 2720 (1991).
[26] R. K. Su, S. D. Yang, and T. T. S. Kuo, Phys. Rev. C **35**, 1539 (1987); H. Q. Song and R. K. Su, *ibid.* **44**, 2505 (1991); H. Q. Song, Z. X. Qian, and R. K. Su, *ibid.* **47**, 2001 (1993); Y. J. Zhang, R. K. Su, H. Q. Song, and F. M. Lin, *ibid.* **54**, 1137 (1996).